available at www.sciencedirect.com

ScienceDirect

www.elsevier.com/locate/matchar



United States Capitol dome: Characterization of cast and wrought materials☆

C.N. McCowan[a,*], T.A. Siewert[a], J.D. McColskey[a], K. Hildebrand[b], D.L. Olson[c]

[a]NIST, Materials Reliability Division, 325 Broadway, Boulder CO, United States
[b]Office of the Architect of the U.S. Capitol, Washington DC, WA, United States
[c]Colorado School of Mines, Dept. of Materials and Metallurgical Engineering, 1812 Illinois Street Golden, CO, United States

ARTICLE DATA

Article history:
Received 21 January 2011
Received in revised form
27 April 2011
Accepted 8 May 2011

Keywords:
Cast iron dome
Gray cast iron
Microstructure
Wrought iron
U.S. Capitol dome

ABSTRACT

Restoration of the cast iron dome at the United States Capitol is needed because moisture is leaking into interior areas of the building due to corrosion damage. Microstructure, composition, and tensile properties of cast and wrought samples from the dome are discussed in this report. The cast iron skin of the dome is a ferrite–pearlite gray iron with strength consistent with the carbon and silicon content. By current compositional and strength requirements the gray iron alloy comes close to meeting requirements for a class 20 gray iron. The microstructure shows good morphology and distribution of Types A and B graphite flakes that are appropriate for the intended service of the castings. In 20–20 hindsight, the decisions made concerning the composition of the iron, and the details of the molding and casting conditions were all quite good. Fatigue data indicate that good performance should be expected to continue for the dome for many years to come.

Published by Elsevier Inc.

1. Introduction

The Office of the Architect of the Capitol began planning restoration of the skin on the cast iron dome at the United States Capitol in 1998. Restoration is needed because moisture is leaking into interior areas of the building due to corrosion damage and cracks in the skin of the Capitol dome. As a part of this planning process, samples of cast and wrought iron from the Capitol dome were examined and various joining procedures for repairing the cracks were evaluated. The microstructures, composition, and tensile properties of cast and wrought samples collected for characterization are discussed in this report. The focus is historical, given the source of the materials evaluated, so brief backgrounds on iron metallurgy and the construction of the dome at the United States Capitol are presented. The microstructures and properties of the material evaluated are then characterized to serve as documentation of these materials in their historical context. The welding-trial results have been published previously [1].

2. Background

2.1. The Dome of the United States Capitol

The dome at the United States Capitol, shown in Fig. 1, was designed in the 1850s by Thomas U. Walter. It was the second-largest cast iron dome in the world when it was built and is currently the world's largest cast iron dome. It replaced an earlier wooden dome that was no longer in scale with the

☆ Contribution of NIST, an agency of the US government; not subject to copyright in the United States.

* *Corresponding author at:* NIST, Division 853, 325 Broadway, Boulder, Colorado 80305. Tel.: +1 303 497 3699; fax: +1 303 497 5939.
E-mail address: mccowan@boulder.nist.gov (C.N. McCowan).

1044-5803/$ – see front matter. Published by Elsevier Inc.
doi:10.1016/j.matchar.2011.05.002

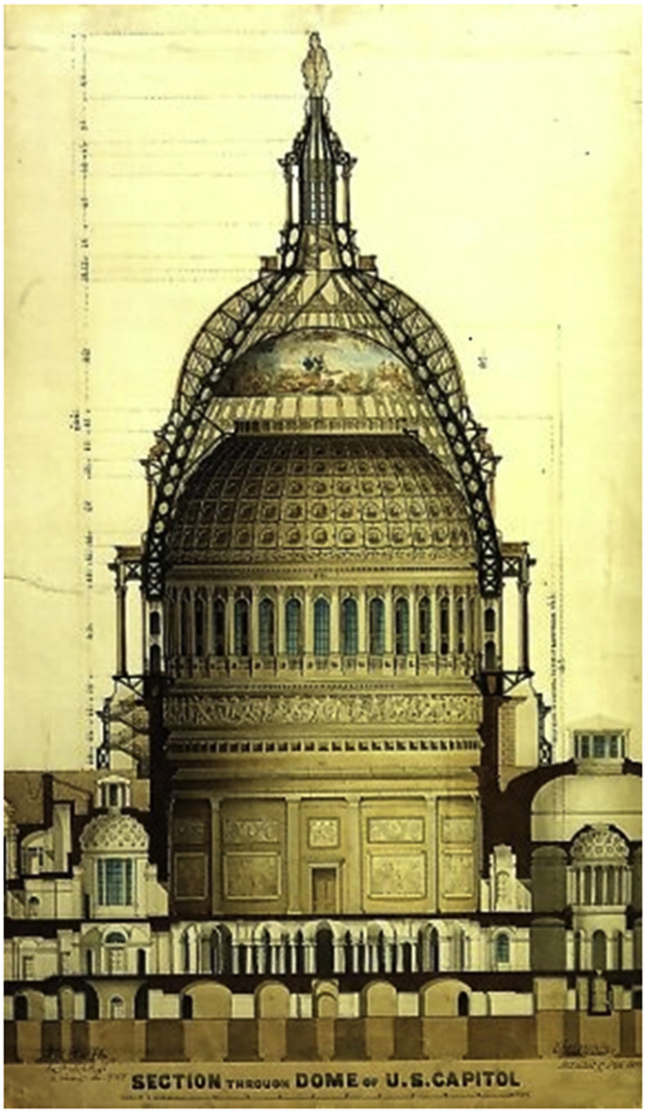


Fig. 1 – Architectural section through the dome of the United States Capitol [3].

expansions needed for the House and Senate wings to accommodate legislators from the states that had just been added to the Union. A cast iron dome was chosen because it could be cast with cutouts in areas where material was not required; it was fire resistant; it could be formed in complex shapes; and it could be erected with pieces of convenient sizes. In 1856, the Baltimore foundry of Poole and Hunt cast the 72 brackets (2774 kg or 6116 lb each) that were used in pairs as cantilever supports for the columns [2]. This work was installed just before the winter of 1857.

The dome itself was cast and installed by Janes, Fowler, Kirtland and Company (Bronx, NY) for fifteen cents per kilogram (seven cents per pound). The project was awarded in 1860, with the agreement that the firm would complete all remaining castings needed for the dome and install them. Construction continued following the outbreak of the Civil War in 1861. Two-thirds of the work was completed on the 4041 t (8.9 million pounds) dome when the Secretary of War called a halt to the work in May of 1861, citing the government's need to finance the efforts of the War of the Rebellion rather than works of art. However, the Janes, Fowler, Kirtland and Company had 590 t (1.3 million pounds) of iron on the site when the Secretary of War advised them not to expect payment for further work until the country's financial situation improved, and they decided to continue work with a reduced workforce to protect their material and investment. Therefore, work on the Capitol never stopped during the war. In 1862, the authority for construction of the dome was transferred from the War Department to the Department of the Interior and work resumed in earnest (with funding). The installation of the dome was completed in 1865 at a reported loss of $125,000, mostly due to increases in cost associated with the one year delay ($60,000 of this loss was reimbursed by the government). The interior work on the dome was completed in 1866.

The dome consists of 36 arched ribs that bear on 36 paired pillars that, in turn, bear on 36 pairs of cast iron brackets embedded in the masonry walls of the Great Rotunda. The ribs are tied together at multiple levels by bands or hoops, consisting of either cast iron sections or wrought-iron riveted plates. From the main rib framing, an elaborate arrangement of cast iron

brackets supports the outer shell of the dome and gives it its distinctive shape. The inner shell is suspended from the main ribs with either wrought-iron hangers or cast iron brackets. At the top of the dome, the 36 ribs converge into 12 ribs that continue upward to support the Tholos and Lantern Levels, and the statue "Freedom." More information on the dome is available at the website of the Architect of the Capitol [3].

The interior rib structure of the dome (the supporting structure) is presently in good condition, but the outer cast iron shell has cracks and visible corrosion at a number of the joints. The water leaks are associated with gaps caused by expansion and contraction of the exterior shell, and failing filler material in the joints between abutting plates. Most of the joints in the exterior skin are lap or butt joints that are difficult to seal. The leakage led to corrosion at the joints of the outer shell and railings (castings or wrought structural forms about 1 cm thick). The corrosion products accumulated in the joints and stressed the component castings beyond what could be accommodated by the mechanical fasteners, leading to cracking of the shell panels and railing components. This situation allows the penetration of more moisture, which promotes still more corrosion.

2.2. *The Family of Cast Irons*

The family of cast irons includes various types of microstructures and properties. Cast iron is a high carbon content ferrous alloy with greater than 2 mass% carbon, which is the highest solubility of carbon in the austenite phase field. To help understand the nature of the irons of the Civil War period, two types of cast iron are introduced.

Traditional cast iron furnaces, especially tall shaft furnaces, pour eutectic liquid of about 4.3 mass% carbon. As illustrated on the iron–carbon phase diagram in Fig. 2, the eutectic composition has a melting temperature which allows it to be poured with a green foundry sand molding practice making this iron product economical. If the silicon content is low, the resulting iron has a ferrite-iron carbide microstructure that has experienced its evolution from the high temperature liquid to an austenite and carbide (Fe_3C) microstructure called ledeburite. On further cooling the eutectoid reaction is experienced, resulting in the austenite transforming into ferrite and an iron carbide microstructure called pearlite. The result is a very hard material called "white iron" due to its cleavage-like fracture giving the fracture surface a white cleavage look. Today, white irons have a range of 1.8 to 3.6 mass% carbon to achieve the best casting properties for load-bearing, abrasion resistant material. This cast iron in its basic elementary form has been poured and used since the 1500s.

The addition of silicon to the iron–carbon melt hinders the formation of iron carbide resulting in the formation of the more thermodynamically stable graphite. In this case, the iron–carbon eutectic results in the formation of an austenite–graphite flake eutectic structure. On further cooling, the austenite is converted to a eutectoid microstructure consisting of pearlite and graphite flakes. This form of cast iron is called gray iron. Its fracture has a gray appearance, because fracture occurs preferentially along the gray colored graphite flakes. Gray iron (and white iron) has a melting, pouring, and molding foundry practice similar to the brass castings. It is this form of cast iron that was used in the U. S. Capitol dome.

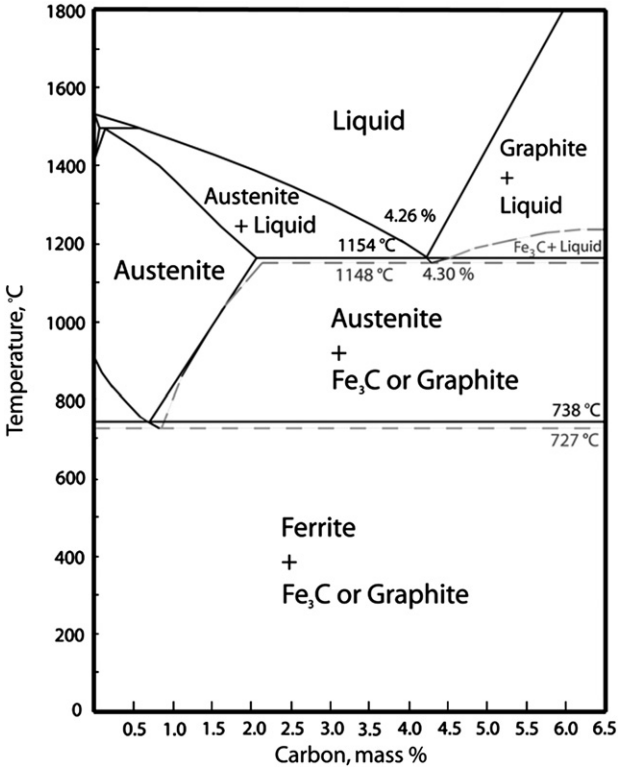


Fig. 2 – The stable iron–carbon phase diagram with the metastable Fe–Fe_3C system in gray dashed lines. Adapted from ASM Specialty Handbook: Cast Irons [9].

Most cast irons in the United States were melted and poured after about 1830 with a continuous cupola shaft furnace. The raw materials were charged at the top, and the molten metal and slag were tapped at the bottom. The alloys were poured at or near the eutectic temperature with the eutectic temperature and composition being altered from that shown in Fig. 2 by the silicon content of the melt. A change in silicon content from 0 to 4 mass%. shifts the eutectic from 4.3 to 3 mass% carbon and increases the eutectic temperature slightly (about 30 °C) [4].

2.3. *Wrought Iron*

Wrought iron of the Civil War era is "worked iron" that is refined to reduce the carbon content. Typically, a drop from 3 to 4 mass % carbon to about 0.02 mass% carbon is achieved through direct oxygen or oxide reduction and production of CO gas. This processing produces iron with approximately 0.02 mass% carbon with a mixture of slag and other impurities. The composite mixture has a sufficient ductile iron matrix to allow for some thermal deformation processing and machining.

Since the 1100s charcoal and iron ore were processed in small bowl or low-shaft furnaces (bloomery) to produce wrought iron in a single-stage (direct) reduction process. Introduction of the taller shaft, forced blast furnaces in the 1400s allowed for development of higher production multi-stage reduction processes. In these furnaces, air was blown into the tuyere of the furnace, which increased the process temperature and enabled ore to be reduced to a molten, high-carbon, pig iron product. Second stage processes, such as fining, were then used to refine

pig iron to a low carbon wrought iron. By the late 1700s a refining process called puddling was a typical refining process for wrought iron [5].

In the puddling process, the pig is re-melted in a shallow hearth and refined by continuous mixing with a slag rich in iron oxide. The refining temperature is below the melting temperature of low carbon iron, so the product was a spongy mass (puddle ball) of iron and slag. The puddle balls were reheated and worked at a temperature where slag is molten, which resulted in further refinement of the metal by squeezing out slag. The final product still contained approximately 400 inclusions per square millimeter (250,000 inclusions per square inch).

By the 1800s wrought iron was a primary industrial material. Typical wrought irons of the 1800 to 1900s varied in composition, but a typical composition, based on fifty specimens with known service history from 1825 to 1922, is shown in Table 1 [6]. Of course, "typical" is not always the most interesting or pertinent information. Some specimens in the 1900's study had compositions with mass fractions as high as 0.06% carbon, 0.07% manganese, 0.37% phosphorus, 0.06% sulfur, 0.33% silicon, and 4.2% slag. So, clearly the variation in composition is significant and often relates to the type of service the steel was produced for, as might be expected. For example, wrought steel produced for hand rail might have much higher slag and impurity content that steel produced for pipe or boiler applications. Wrought iron is known for good corrosion resistance, and bars with diameters of less than 40 mm might have a tensile strength near 330 MPa, yield strength near 200 MPa, elongation over 20%, and reduction in area of near 40%.

3. Experimental Procedures

3.1. Metallographic

Metallographic specimens were taken from circular coupons that had been removed from the dome during the installation of new rainwater drains, and parts from a railing and a gutter that had been replaced in the past. The specimens evaluated here are therefore not necessarily optimal for sampling the structure, but they represent a cross section of the materials used to construct the dome at the United States Capitol.

Preparation of samples for light and scanning electron microscope evaluation followed typical procedures recommended in the literature [7]. SiC grinding papers were used for coarse and fine grinding operations. Vibratory polishing with colloidal silica was used for selected specimens. Specimens were etched using several etchants and combinations of etchants. The etchants used for particular specimens are noted in the figure captions.

Table 1 – Typical composition (mass %) for American made wrought irons of the late 1800's and early 1900's.

	Combined analysis	Base metal	Slag
C	0.02	0.02	
Mn	0.03	0.01	0.02
P	0.12	0.10	0.02
S	0.02	0.02	
Si	0.15	0.01	0.14
Slag	3.00		

3.2. Composition

Specimens from three different castings on the skin were sent out for spectroscopic analysis. All three specimens were analyzed for carbon, manganese, silicon, phosphorous, and sulfur. One specimen was also analyzed for chromium, nickel, molybdenum, copper, aluminum, and titanium. Compositional analysis of microscopy specimens was conducted on polished surfaces with energy dispersive X-ray spectroscopy (EDS) in a scanning electron microscope.

3.3. Tensile and Fatigue

Tensile and fatigue specimens were taken from a gutter section, with a width of about 115 mm. The width limited the length of the tensile specimens, and resulted in reduced-section specimens. The specimens were machined to the sheet-type specimen dimensions for "Rectangular Tension Test Specimens" (according to ASTM Standard E-8), with an exception for length and the use of clamp grips rather than pin grips [8].

The faces of the specimens were machined just enough to remove the surface damage, which resulted in final thicknesses near 7 mm. The specimen width was machined to 12.5 mm, producing cross-sectional areas near 90 mm^2. Because of the low ductility expected for cast irons, the strain was measured by strain gages bonded to the machined faces.

A servohydraulic test machine was used to apply a sinusoidal load spectrum for fatigue testing. The ends of the specimens were clamped, then cycled between minimum and maximum tensile loads. Based on the low cyclic loads (mostly due to thermal expansion) on the dome, the maximum load was set just above the first deviation from elastic behavior (about 25 MPa or 4 ksi), a load thought to represent the intensity of variable loads on the dome due to snow, wind, and thermal cycles. The load was cycled between the maximum load and half this load until fracture (an R ratio of 0.5).

4. Results and Discussion

4.1. Chemical Composition of Cast Iron Samples

Cast irons have carbon contents above a mass fraction of 2%, which distinguish them from steel. Carbon, silicon and manganese are the primary alloying elements, but morphology of the microstructure is also influenced by trace elements. Compositions for three specimens evaluated in this study are given in Table 2.

Table 2 lists the results of spectroscopic analysis for three specimens taken from different castings on the skin of the dome. Variations in the compositions are likely due to slightly different formulations and ores used over the duration of the project, and to adjustments made to the melts to increase the liquidity and casting quality.

The compositions of the samples evaluated in Table 2 show that both the carbon and silicon contents of the iron are at the

Table 2 – Compositions of three specimens from different gray iron castings on the dome at the United States Capitol, in % mass fraction.

Element	Specimens		
	A	B	C
C	3.36	3.62	3.86
Mn	0.67	0.82	0.48
Si	3.20	2.18	2.31
P	0.78	0.82	0.60
S	0.11	0.08	0.06
Cr			0.01
Ni			0.04
Mo			0.01
Cu			0.02
Al			0.001
Ti			0.11
CE	4.7	4.6	4.8

high end of the compositional range expected for modern gray irons (range in mass fraction of 2.5 to 4.0% carbon and 1.0 to 3.0% silicon) [9]. The mass fraction is near the range of 3.4 to 3.6% carbon and 2.3 to 2.5% silicon that is specified for a class 20 Gy iron. As a general rule, increased carbon and silicon contents result in decreased strength, but a balance of factors are important for the dome. General castability is likely the most important consideration for the dome, where increasing carbon increases fluidity, and the combined alloy content helps to ensure full graphitization of the gray iron throughout the cross section of the thin castings poured for the skin of the dome.

Table 2 also includes a value for carbon equivalence (CE). This term is used to estimate if a cast iron composition will solidify in a hyper or hypoeutectic mode, which are terms used to describe if solidification starts above or below the eutectic composition on the iron–carbon phase diagram (a mass fraction of 4.3% carbon). While many different formulas have been developed to compute the carbon equivalence, a simple version is given in Eq. (1) [8]:

$$CE = \%C + \frac{\%Si + \%P}{3} \quad (1)$$

This equation for carbon equivalence indicates that both silicon and phosphorus function like carbon in determining the microstructure, but at one third its effectiveness. The cast iron from the skin had CEs from 4.6 to 4.8, which are well above that of the eutectic composition of 4.3. All three specimens evaluated are hypereutectic alloys.

The phosphorus contents for the three specimens range in mass fraction from 0.6 to 0.8%, which is within the range expected for unalloyed gray iron (0.002 to 1.0%). Modern gray irons often have mass fractions of 0.02 to 0.2% P [9]. However, phosphorus is not an alloy addition. It is present in the pig used to make the gray iron. It forms a phase called steadite, which is an iron–phosphorus low melting point eutectic. This phase is one of the last phases to solidify and it hardens the matrix (for improved wear resistance).

The manganese mass fraction of 0.1 to 1.0% is within the range expected for gray iron historically, but is a bit low by today's expectations [9]. Manganese is added to combine with sulfur and keep it off of the grain boundaries, where it can reduce the ductility of the casting. From Eq. (2),

$$Mn > 1.7S + 0.3 \quad (2)$$

the manganese content required to keep the grain boundaries clean for specimen A is 0.49, which is low compared with the mass fraction measured of 0.67% Mn. A similar result is found for specimen B, where calculated and measured manganese mass fractions were 0.44% and 0.82% respectively. For specimen C, the calculated and measured manganese mass fraction are closer to predicted by Eq. (2) (0.40% calculated and 0.48% measured). In all cases, manganese additions appear sufficient considering sulfur contents.

The sulfur contents are within the range currently expected for unalloyed gray iron. Sulfur content can be as high as 0.15% in "low quality" gray irons and is significantly lower in high quality gray iron [9]. In either case, sufficient manganese is needed to protect the grain boundaries.

Compositions of the rib casting from the dome at the United States Capitol were reported in the 1998 report [10]. The ribs, which require different mechanical properties than the skin casting, had a CE of 3.9 mass%. This composition is well below that of the eutectic composition (hypoeutectic) and indicates that differences in the structures between the rib and skin castings should be expected.

4.2. *Chemical Composition of the Wrought Iron*

The wrought iron specimen evaluated in this study was analyzed for chemical composition with EDS to estimate the manganese, phosphorus, silicon, and sulfur contents. The compositions of these elements, in mass fractions, were 0.9% Mn, 0.62% P, 0.3% Si and 0.3% S. For comparison, a wrought iron specimen (0.025% C) taken from a plate at the Capitol dome and evaluated in the 1989 study was reported to have a mass fraction of 0.13% Mn, 0.13% P, 0.10% Si,, and 0.01% S, which is an alloy of higher quality [10]. Neither example quite meets the general expectation of a good-quality puddled wrought iron having less than 0.08% C, 0.10% Mn, 0.04% P, 0.10 Si%, and 0.05% S [11]. But, as American historical data show, compositions vary and wrought steel that did not need to qualify as a "good quality" can vary significantly from these expectations [6].

4.3. *Mechanical Properties of Cast Iron*

The tensile strength of the cast iron was evaluated using a piece of a gutter because the other available samples were too small.

The dual displacement strain measurements (front and back) were designed to detect bending, after the relatively low elongation value was observed for the first specimen tested. Bending would have a relatively large effect on the measurement of small elongations, and the excellent correspondence between the data for the fronts and backs of the other specimens confirmed that little bending occurred.

These tensile strength data compare well with the values calculated in the 1998 study from hardness measurements on the ribs and with the tensile strengths measured for the rib castings: 120 to 130 MPa [10]. The rib castings have slightly lower

strength than the castings evaluated here, and are distinctly more ductile.

The strength measurements compare well with predictions based on compositions and microstructure [12]. The high carbon equivalent that helped to increase the fluidity during the casting operation also reduced the strength of the castings. Increasing the carbon equivalent from 3.5 to 4.5 in gray iron castings is predicted to lower the tensile strength from about 350 to 150 MPa.

No yield strengths are reported for the specimens, because all specimens failed before or just after meeting the 0.2% offset plastic criterion of ASTM E 8. However, the strain gages provided an accurate measure of the strain to failure, which ranged from 0.17% to 0.25%. The plastic strain did not appear suddenly after a period of elastic loading. It occurred gradually and progressively as the load was applied. The curves began to deviate from a straight line at very low loads, perhaps as low as 25 MPa (4 ksi). Thus, tensile damage begins to accumulate at very low stresses (about 20% of the ultimate strength), and this confirms that the dome is sensitive to the slight bending or tensile loads associated with a buildup of corrosion products in the joints. Several unloading cycles during the tensile tests provided a rough estimate of the modulus of around 83 GPa. This estimate is in line with the tensile modulus reported for class 20 Gy iron of 66 to 97 GPa [9].

Some of the structure of the dome is in compression, so one uniaxial test was performed in compression. The ultimate compressive strength of the specimen tested was about 540 MPa (77 ksi) at a strain of about 1.6%. These values are only approximate, because the specimen started to buckle at this point, making further analysis complicated. However, the result shows that the gray iron is at least twice as strong in compression as in tension, and it has greater ductility. Thus, the tensile values can be nearly doubled for modeling of compression applications. The application of cast iron for compression members and wrought iron for tension members indicates recognition of these characteristics by the designers of the dome, and helps to explain its good performance over the years.

Fatigue testing showed encouraging results, as seen in Table 3. Below maximum tensile loads of 105 MPa (15 ksi), the fatigue specimens were still intact and crack-free up to 180,000 cycles. The tests were terminated after this value because it corresponds to about 500 years of daily thermal cycles (caused by the usual day to night temperature swings). Since the dome has experienced only a small portion of this life, there should be ample remaining life for loads at this level. In addition, most of the loads on the dome are expected to be compressive, so these test results would be conservative estimates of compression fatigue behavior. Only once at 105 MPa did we note a fracture, and then only after 60,000 cycles.

Table 3 – Fatigue data from cast iron specimens taken from the skin on the dome of the United States Capitol.

Max load (MPa)	Min load (MPa)	Cycles to failure
35	17.5	>180,000
70	35	>180,000
105	53	60,000
105	53	>180,000
140	70	>180,000

This failure initiated at a 2 mm deep corrosion pit on the surface of the specimen. Additional specimens at 105 MPa and at 140 MPa were still intact and free of cracks up to 180,000 cycles.

4.4. *Microstructure of Cast Iron Skin of the Capitol Dome*

The skin castings from the dome contained graphite flake morphologies that are representative of both flake (Type A) and rosette (Type B) structures. The Type A flakes are relatively large and are dispersed randomly, compared with Type B flakes, which form in clusters referred to as rosettes that have smaller individual flakes. The Type B graphite structure is formed in near-eutectic compositions and is promoted by higher cooling rates, such as those common to castings with section thicknesses below about 10 mm (like the skin castings). The size of the rosettes reflects local cooling conditions because each rosette is a single eutectic solidification cell, and smaller cells are associated with fast cooling rates.

Fig. 3a shows a region from a skin casting that has both rosettes and randomly oriented flakes between the rosettes. The size of the rosettes here are on the order of 200 μm. The randomly oriented Type A graphite flakes (Fig. 3b) in the specimens were typically near 100 μm in length, which is well below the maximum length of 160 μm expected for Type A flakes. A fine graphite flake structure is common for hypereutectic gray iron and would be expected to provide mechanical properties appropriate for the skin.

The various specimens evaluated from the skin castings show different ratios of Types A and B graphite structures, varying from solely Type A to solely Type B. Such variation in microstructure is expected for castings produced over time, possibly by different foundries, especially when the section thickness is near the transition of Type A to Type B cooling conditions.

The anisotropic structure of the Type A graphite flakes is visible in Fig. 3c and d with cross-polarized light. Graphite lamellae often have curved shapes, with single crystalline structures over significant regions of their length. The lamella grows primarily at its edge, with thickness hardly increasing due to difficulty in growth along the c-axis, which is normal to the lamella [13]. Details of the anisotropic lamellae within the Type A graphite flakes show that lamellae are often aligned over long regions. However, graphite structures within branches of the lamellae, and sometimes within the flakes, can show complex orientations.

Manganese sulfides are visible in the as-polished microstructure in Fig. 3. These inclusions are gray and angular. The inclusions are formed when manganese additions are made to the alloy to help increase the ductility of the casting by preventing elemental sulfur from collecting at boundaries in the microstructure.

In Fig. 4a–d, details of the microstructure of the skin castings are shown. As the casting cooled from the liquid, the graphite flakes formed along with austenite, using up much of the iron, carbon, and silicon in the melt. Finally, the only liquids left had the composition of the low-melting-point eutectics (Fe-C and Fe-P). As these final liquids solidified, they filled in the gaps between the austenite grains. As the solidified casting cooled further, some of the remaining carbon diffused to the carbon flakes and the austenite transformed to a mixture of ferrite and pearlite.

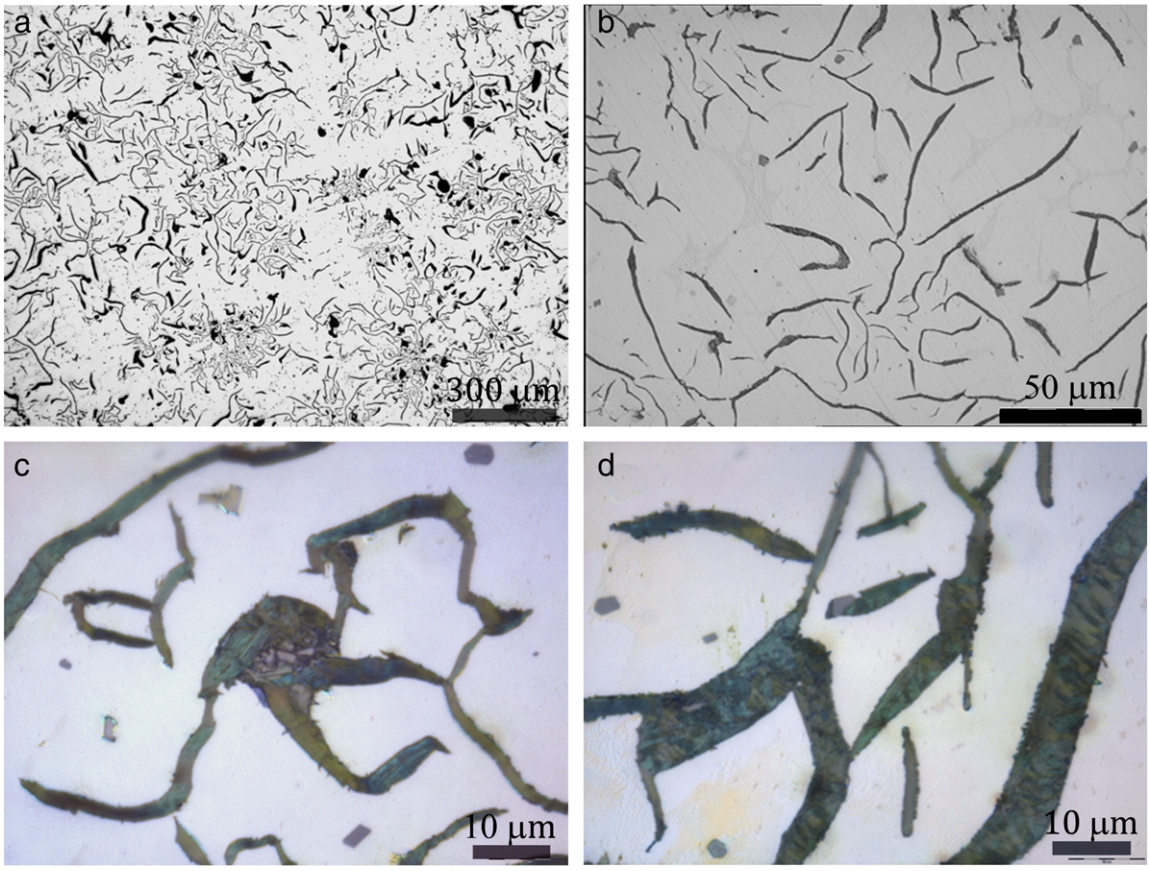


Fig. 3 – Graphite flake morphologies typical of the skin on the U.S. Capitol dome: (a) as-polished, showing mostly type B rosette graphite structures, (b) as polished showing mostly type A graphite flakes, (c) internal structure of graphite with cross-polarized light, and (d) internal structure of graphite flake under cross-polarized light.

The microstructure that surrounds the graphite flakes in Fig. 4a–d is often free ferrite in the skin casting. Pearlite, which is a structure of alternating lamellae of ferrite and iron carbide, is typically associated with the phosphorus rich eutectic structure (Fe-P). This mixture of matrix phases was common in the samples evaluated here, and the microstructure is likely best described as ferrite-pearlitic gray cast iron. It has many regions that are predominantly pearlitic gray cast iron, indicating a pearlite matrix, but ferritic regions are also common in the specimens. As expected for ferrite-pearlitic cast iron, the ferritic matrix regions (blue or green in the figure) are associated with rosette structures in the casting which mark the eutectic cells. The cells are enriched in silicon due to microsegregation and this promotes ferrite formation. The pearlitic regions are colored brown in the lower magnification examples. It was common, even in the more pearlitic regions, to find free ferrite adjacent to the graphite flakes. Compared with many modern published microstructures for gray irons, these microstructures have a lot of ferrite, which would be expected to reduce the strength and increase the ductility compared with a fully pearlitic matrix. However, if the ferrite is principally promoted by silicon enrichment, rather than slow cooling rate, the ferrite would be expected to be strengthened and could have lower ductility than expected. In the higher magnification examples in Fig. 4(c) and (d), the free ferrite around the graphite flakes is apparent, and fine pearlitic structures (lamellae) are adjacent to the Fe-P eutectic phase (white) in the microstructure.

The low melting point Fe-P eutectic phase, called steadite, is shown with two etches in Fig. 4c and d. Steadite is often found in gray iron with phosphorus contents greater than 0.02 mass%. It is uncolored by the etchants, but the lower contrast obtained between the steadite and the matrix with the Klemm's reagent is helpful when evaluating details of the steadite phase [7,8]. Steadite has a striking appearance in the microstructure, but offers little advantage in this application. It is a hard phase, as indicated by the relief in the microstructure of the as-polished specimens in Fig. 3b, and can offer improved wear resistance for some applications. The steadite and pearlite structures mark the interdendritic and intercellular regions in the microstructure of the skin casting because, as previously mentioned, these eutectic structures are the last to solidify from the melt.

As a final point in this section, an example of martensite formation in the gray cast iron from the Capitol dome is shown in Fig. 5. This martensite formed in the heat affected zone of a weld made to study joining procedures that might be used to repair cracking in the cast iron dome. Repair techniques considered typically involve welding or brazing, and the heat affected zones associated with the various techniques result in changes to the microstructure and residual stresses that can

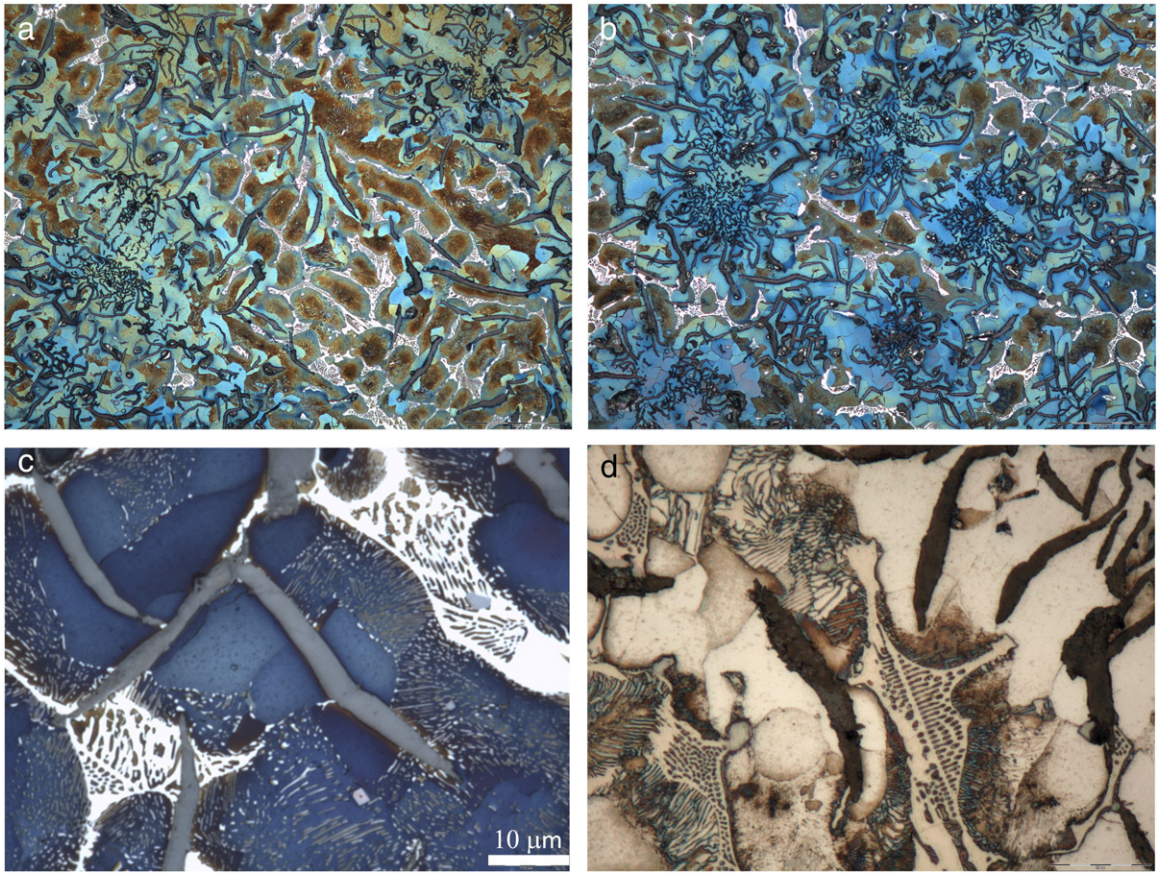


Fig. 4 – Microstructure of the skin castings shown with Beraha's etch in a–c, with pearlitic regions in brown, steatite in white, ferritic regions in blue, and graphite in black. In d, a similar region to c has been etched with Klemm's etch, which reduces the contrast between steadite and ferrite.

result in cracking. Clearly the principal change in the microstructure of Fig. 5 is due to the formation of martensite during the cooling cycle of the weld. Plate martensite structures fill the inside of eutectic cells regions bounded by regions of steadite. Some martensite can be tolerated in the microstructure, but it must be limited using appropriate welding process and procedures so that the microstructure can tolerate the residual stress (and applied stress in service) and avoid cracking.

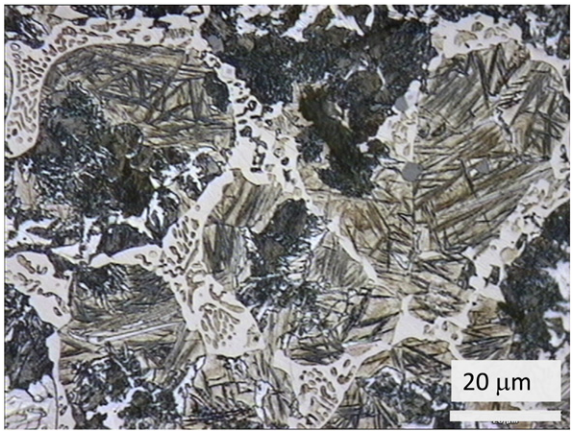


Fig. 5 – Optical micrograph of martensite formed during a weld cooling cycle, obtained with Beraha's etch.

4.5. *Microstructure of Wrought Iron*

The microstructure of a wrought iron plate from the Capitol Dome is shown in Fig. 6. The principal features of the microstructure are ferrite grains and large, often complex, inclusions. The wrought steel contains so many inclusions that it is composite-like. The inclusions are introduced to the relatively inclusion free pig during the second stage of the refining process, puddling. In this stage, slags are mixed by hand with the molten pig iron to reduce carbon, silicon, sulfur, phosphorous and manganese contents. Assuming this wrought iron was made in or around the mid 1800s, puddling had been in use for centuries and steel was just starting to be refined with Bessemer converters.

The microstructure has equiaxed ferrite grains (Fig. 6f). The color etch consistently showed both the current ferrite grain boundaries and a ghost boundary structure (white). The ghost structure has a morphology and size distribution that is very similar to the current ferrite grain structure and is presumed to mark prior grain boundaries where segregation occurred.

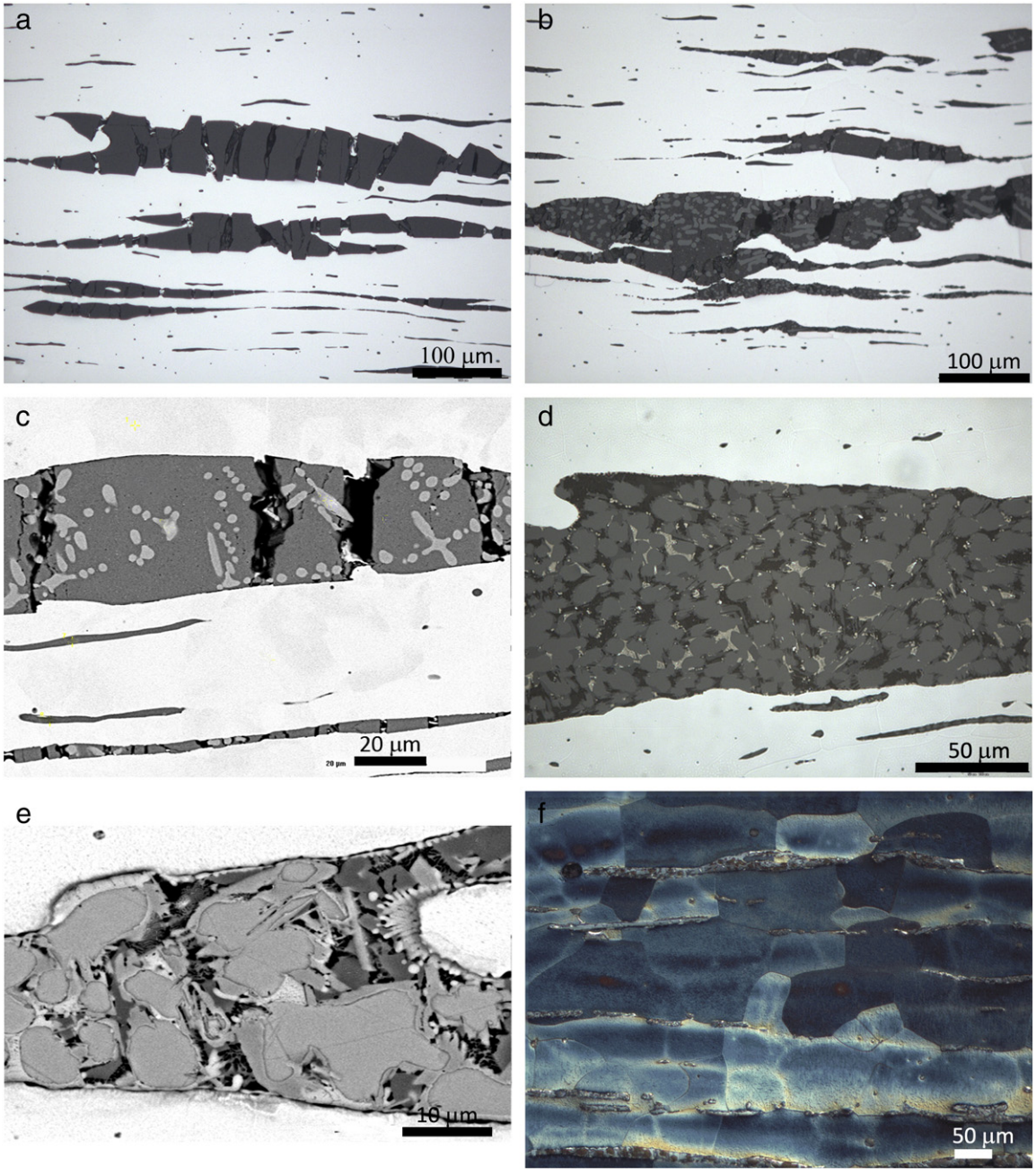


Fig. 6 – Inclusions and ferrite grain morphology in a wrought steel for the Capitol dome. The micrographs show: (a) light microscope image of a large single phase inclusion, (b) light microscope image of a large dual phase inclusion, (c) light micrograph of a multi-phase inclusion, (d) scanning electron micrograph of a multi-phase inclusion, (e) scanning electron micrograph of a very complex inclusion, and (f) light micrograph with Beraha's etch showing inclusions and ferrite grains.

The ghost structures are often associated with phosphorous segregation in puddled wrought iron. However, these ghost structures are described in the literature as being associated with phosphorus and non-phosphorus-rich regions in the ferrite, and not necessarily associated with grain boundaries [14]. The color etch also shows other indications of segregation in the structure along rolling (work) planes and inclusions. The ferrite grain structure is separated by a multitude of dark horizontal lines, which are slag islands (inclusions). Details of various types of slag inclusions common to the wrought iron are also shown in Fig. 6a–e.

At higher magnifications, details of the inclusions become apparent. Some inclusions are simple single phase inclusions, but most are more complex. The single phase inclusions observed in this steel are typically fractured into angular shapes that indicate low ductility (Fig. 6a). They are oxides rich in iron and silicon, like fayalite (Fe_2 SiO_4), with some manganese, phosphorus and sulfur. Most typical of puddled

iron are the two-phase wüstite-rich slags (FeO) shown in Fig. 6b and c. The iron-rich phase is characteristically recognized by the rounded dendrite morphology and light color, with respect to the matrix. The matrix is an oxide rich in silicon and manganese, with some calcium, phosphorus, and sulfur. One example of a three-phase wüstite-rich slag is given in Fig. 6d. In this example the lightest colored phase has an appearance like the Fe-P eutectic phase, but it is low in phosphorus. (Carbon content was not analyzed, but the phase appears to be an oxide phase with some manganese, and small amounts of molybdenum, silicon and phosphorus.) The phosphorus rich region in this example is the darkest phase. The lighter colored matrix phase is wüstite. The final example of a slag inclusion is a very complex inclusion indeed (Fig. 6e). This inclusion is even more complex than it looks, in that phases having very similar contrast (color) do not all have the same composition. It suffices to say that this inclusion has two oxides rich in phosphorus, three rich in silicon, one rich in calcium (one of the phosphorus-rich phases), one phase rich in sulfur, and others. The sulfur-rich phase is recognizable as having a type II dendritic sulfide morphology, adjacent to the lightest colored phase in the inclusion.

5. Summary and Conclusions

The cast iron skin of the dome has performed well for over 145 years. This is not surprising in that it was constructed during a heyday in cast iron architecture when quality of casting companies, practical knowledge, and skilled labor for cast iron construction were all high. The cast iron skin is a ferrite–pearlite gray iron with strength consistent with the carbon and silicon contents. By current compositional and strength requirements, the gray iron alloy comes closest to meeting requirements for a class 20 Gy iron. The microstructure shows good morphology and distribution of Types A and B graphite flakes that are appropriate for the intended service of the castings. Therefore, in hindsight, the decisions made concerning composition of the iron, the details of the molding and casting conditions, and the overall design of the dome were all quite good. Fatigue data indicates that good performance should be expected to continue for the dome for many years to come.

The wrought iron specimen evaluated is a composite structure of ferrite grains (no pearlite) and slag inclusions. The specimen is an example of a refinement quality acceptable for use as handrails and other non-critical applications. Segregation and ghost boundaries were apparent, as might be expected for a wrought iron product of the mid 1800s. Inclusions varied greatly in size, morphology, and composition, which is typical for a hand puddled wrought iron.

REFERENCES

[1] Siewert T, McCowan C, Bushey R, Robinson B, Christ T, Hildebrand K. Preserving a national landmark. Weld J November 2000;79(11):55–60.
[2] Allen WC. History of the Capitol dome. Washington: U.S. Government Printing Office; 2001.
[3] http://www.aoc.gov.
[4] Heine RW, Loper Jr CR, Rosenthal PC. Principles of metal casting. second edition. McGraw-Hill; 1967.
[5] Samuels LE. Optical microscopy of carbon steels. Metals Park, Ohio: American Society for Metals; 1980.
[6] Aston J, Story EB. Wrought iron: its manufacture, characteristics, and applications. Pittsburg, Pennsylvania: A. M. Byers Company; 1939.
[7] Radzikowska J. Preparation of cast iron foundry alloys. Tech-Notes 1998;2(2).
[8] ASTM Standard E8. Standard E8 standard test methods for tension testing of metallic materials. West Conshohocken, PA: ASTM International; 2000.
[9] Davis JR, editor. ASM specialty handbook: cast irons. Materials Park, OH: ASM International; 1996.
[10] Pitkin L. United States Capitol dome structural member assessment — Washington, D.C., report M98028; July 14 1998.
[11] Samuels LE. The metallography of a wrought iron anchor from the Bark Endeavor. Metallography 1980;13:357–68.
[12] Properties and selections: iron, steel, and high performance alloys, metals handbook. Metals handbook, Tenth Edition Materials Park, Ohio: ASM International; 1990. p. 3–32.
[13] Lux B, Vendl A, Hahn H. Review on the formation of microstructures in gray iron. Cryst Res Technol 1981;16(5): 531–56.
[14] Buchwald VF, Wivel H. Slag analysis as a method for characterization and provenancing of ancient iron objects. Mater Charact 1998;40:73–96.